Efficiency Calibration of the DSS 13 34-Meter Diameter Beam Waveguide Antenna at 8.45 and 32 GHz

S. D. Slobin
Telecommunications Systems Section

T. Y. Otoshi, M. J. Britcliffe, L. S. Alvarez, S. R. Stewart, and M. M. Franco
Ground Antennas and Facilities Engineering Section

Efficiency measurements at 8.45 and 32 GHz (X- and Ka-bands, respectively) have been carried out on the new 34-meter diameter beam waveguide antenna now in use at the NASA Goldstone Deep Space Communications Complex. The use of portable test packages enabled measurements at both the Cassegrain and beam waveguide focal points. Radio sources (quasars and Venus) were used as calibrators, and updated determinations of flux and source size correction were made during the period of the measurements. Gain and efficiency determinations as a function of elevation angle are presented, and the effects of the beam waveguide system and antenna structure are clearly seen. At the beam waveguide focus, an 8.45-GHz peak efficiency of 72.38 percent was measured; at 32 GHz, 44.89 percent was measured.

I. Introduction

From July 1990 through January 1991, the new 34-meter diameter beam waveguide (BWG) antenna at the NASA Goldstone Deep Space Communications Complex in the Mojave Desert was tested as part of its post-construction performance evaluation. This research and development antenna, designated Deep Space Station 13 (DSS 13), is the prototype for a new generation of Deep Space Network (DSN) antennas utilizing the BWG-type of antenna feed system. Figure 1 shows the mechanical and microwave optics designs of the antenna.

Efficiency and pointing performance were characterized at 8.45 and 32 GHz (X- and Ka-bands, respectively) at both the Cassegrain (f1) and BWG (f3) focal points. The f1 focal point is located close to the vertex of the main reflector, while the f3 focal point is located about 35 meters and six additional reflectors away in a subterranean pedestal room. The BWG type of design enables the simultaneous use of numerous different feeds in the relatively well-controlled conditions of the pedestal room, as contrasted with the present DSN configuration with feedhorns, waveguide components, and low-noise amplifiers installed above the surface of the dish, where maintenance and modification tasks are considerably more difficult. In addition, increased system noise temperature due to rain on the feedhorn covers and dichroic plates has been eliminated.

The performance evaluation methods described in this article are unique in that a direct experimental measurement was made of the antenna efficiency and gain degradation caused by the BWG mirror system. The tests in-

volved the use of X- and Ka-band portable test packages that were installed at either focal point f1 or f3. To the authors' knowledge, this is the first known use of portable test packages to determine gain and efficiency at various locations in the microwave optics path of an antenna.

Section II of this article presents the boresight measurement technique and pointing correction methodology used in looking at calibration radio sources of both known and unknown flux and source size correction values. Section III describes the methodology of antenna efficiency determination. Section IV presents methods for atmospheric attenuation correction. Section V presents characteristics of the radio sources used during the boresight measurements. The last sections present the results of the measurements and final deduced values of flux and source size correction for the not-well-known calibration radio sources.

II. Boresight Technique

Critical to the proper performance of the measurements was the use of a boresighting procedure to accurately point the antenna at the radio sources used in the calibration process. The method used was a seven-point boresight technique. This method moved the antenna sequentially in both the cross-elevation (XEL) and elevation (EL) directions both on and off the source. In each direction, the antenna was positioned off-source ten half-power (one-sided) beamwidths; one half-power beamwidth at the 3-dB point; approximately 0.576 half-power beamwidth at the 1-dB point; on source; and then similar offsets on the other side. For example, at X-band with the 34-meter antenna, the full 3-dB beamwidth is 65 mdeg. The offsets used were 325, 32.5, 18.7, and 0 mdeg in each direction. At Ka-band, with a full 3-dB beamwidth of 17 mdeg, the offsets were 85, 8.5, 4.9, and 0 mdeg.

For each scan, an off-source baseline is generated from the two off-source points. A Gaussian curve (relative to the baseline) is fitted to the five remaining on-source points and the peak value of the curve is calculated. Also, the position of the peak is calculated as a measure of the pointing error for that scan. One pair of scans (one XEL and one EL) is considered to be one measurement or data point. The seven pointing offsets for each new scan are corrected for pointing errors found from the previous similar scan, in order to maintain pointing throughout a track. As an example, if for a particular a priori pointing model installed in the antenna control subsystem it is found that from boresight-to-boresight a consistent +3-mdeg pointing error is found in the elevation scans, then this correction is made from scan-to-scan in order to maintain pointing. After 10 boresights, a 30-mdeg total pointing error relative to the model will have been found, although the scan-to-scan pointing error will not exceed 3 mdeg. For the purposes of the efficiency measurements, it is thus assumed that perfect pointing is maintained for all scans and that the small *calculated* pointing errors are due to random errors in the system operating noise temperature measurements, rather than due to *actual* mispointing. No efficiency corrections for any small pointing errors were made in these measurements. Obviously bad data points were discarded.

Two data files are generated during the measurements: an efficiency file and a pointing file. The efficiency file consists of time, antenna azimuth and elevation, and XEL and EL estimates of half-power beamwidth, peak-source noise temperature contribution, and scan pointing error. The pointing file consists of time, antenna azimuth and elevation, and pointing correction. Pointing correction is a cumulative value calculated from the sum of the pointing errors determined from the previous boresights. For example, if the first three boresights found +3, +2, and +4 mdeg pointing errors (relative to the a priori pointing model) in the elevation scans, the total accumulated pointing correction needed after the third boresight would be −9 mdeg. This correction is used in the generation of a new systematic pointing-error correction model for use in future measurements. With a perfect pointing-error correction model, the scan-to-scan pointing errors would be small and of random sign.

This boresight technique was developed at the Jet Propulsion Laboratory as a computer-assisted interactive program utilizing simultaneous operation of a personal computer and the antenna local control and display (LCD) console for pointing the antenna, determining and entering pointing offsets, entering noise temperature data, calculating radio source peak-noise contribution, and determining antenna pointing errors.

III. Antenna Efficiency Determination

For a radio source of known flux density, the increase in system noise temperature as determined by the boresight measurements is a measure of the antenna efficiency. As defined here, the efficiency is referenced to the input of the low-noise amplifier (cooled high-electron-mobility transistor, HEMT) and includes the losses of the feed system. Alternative methods specify efficiency at the aperture of the feedhorn or at the antenna aperture itself. The term aperture efficiency refers to antenna gain relative to that of a uniformly illuminated circular aperture having the same diameter as the antenna, e.g., a 70-percent efficient antenna has 1.549-dB less peak gain than does the circular aperture.

The radio-source noise temperature increase measured by the antenna is given by [1]:

$$\Delta T = \frac{\eta S A}{2kC_r C_p}$$

where

η = antenna aperture efficiency

S = radio source flux, watts/m^2/Hz

A = antenna area, m^2

k = Boltzmann constant, 1.38062×10^{-23} J/K (Wsec/K)

C_r = source size correction, typically 1.0 for point sources, up to ~1.5 for extended sources, including planets

C_p = pointing correction, assumed = 1.0

The flux, S, is typically given in units of "Janskys," where 1 Jansky (Jy) = 1×10^{-26} W/m^2/Hz.

Measured ΔT is compared with the quantity $[(SA)/(2kC_r)]$ to give antenna efficiency. Thus:

$$\eta = \frac{\Delta T}{SA/2kC_r}$$

$$= \frac{\Delta T}{T100/C_r}$$

$T100$ is what would be measured by a perfect antenna looking at a point source emitting the same flux as the observed radio source. C_r is a function of the source structure at a particular frequency and the antenna pattern of a particular antenna at that frequency. For a particular antenna, frequency, and radio source, the $T100/C_r$ can thus be specified.

For a planet, the flux is determined from the blackbody disk temperature and the angular size of the source (which changes as the distance between Earth and the planet changes).

The flux is given by [2]:

$$S = \frac{2kT\Omega}{\lambda^2}$$

where

k = Boltzmann constant

T = blackbody disk temperature, K

λ = wavelength, m

Ω = solid angle subtended by source = $(\pi D^2)/(4R^2)$

D = planet diameter, km

R = distance to planet, km

IV. Correction for Atmospheric Attenuation

ΔT is an on–off source measurement, and the Earth's atmosphere attenuates the true source contribution that would be measured under vacuum conditions. The total atmospheric attenuation was estimated from surface weather conditions during all measurements. The surface temperature, pressure, and relative humidity at the site were recorded every half hour. Typical zenith values of attenuation at Goldstone under average clear-sky conditions are:

$$\text{X-band} : A_{zen} = 0.035 \text{ dB}$$

$$\text{Ka-band} : A_{zen} = 0.115 \text{ dB}$$

The attenuation in decibels at elevation angle θ is modeled as:

$$A(\theta) = \frac{A_{zen}}{\sin(\theta)}$$

The loss factor at that elevation angle is:

$$L(\theta) = 10^{A(\theta)/10}$$

The "vacuum ΔT" then becomes:

$$\Delta T = L(\theta)\Delta T \text{ measured}$$

V. Radio Source Flux Values and Size Corrections

At both X- and Ka-bands, radio source 3C274 (Virgo A) is considered a principal calibrator, although at Ka-band, Venus is considered well-known enough to be used as a primary source also. At both X- and Ka-bands, the principal calibrators are used to establish the peak antenna efficiency near the antenna rigging angle (40–50 deg

elevation). As these sources typically do not rise to high elevation angles, other sources which do are also used to establish the shape of the efficiency curve with the elevation angle. High declination sources, such as 3C84 and 3C123, are used for this purpose. As their fluxes are not well-known (or the sources are variable), the efficiency curves generated are normalized to the peak values determined by the principal calibrators.

Table 1 summarizes the flux, size correction, and other factors associated with the radio source calibrators used during the DSS 13 X-band calibration measurements. It should be noted that radio sources 3C84 and 3C273 are known to be variable; however they are point sources and are useful for pointing model development.

VI. Efficiency Measurements: X-Band at f1, September 1990

By using the peak efficiency value determined by 3C274 to define the antenna performance, it was found that the efficiencies as determined by the other sources (using the $T100/C_r$ values above) varied by as much as 40 percent. Adjustments were made separately to the data points of each source to normalize their curve-fitted peak values to the 3C274 curve-fitted peak value. Table 2 gives the required efficiency adjustments and the deduced flux and $T100/C_r$ values thus obtained. In the case of point sources (3C84, 3C273), the adjustment reflects a flux error. For non-point or extended sources (DR21, 3C123) the adjustment could be due to either flux or source size-correction errors (which are at present unable to be separated); thus only the deduced $T100/C_r$ value is given. It should be noted that the variable sources (3C84, 3C273) may vary considerably over a period of weeks, thus the $T100/C_r$ values found represent, at best, interim values.

The zenith atmosphere attenuation corrections made during these measurements ranged from 0.036 dB to 0.046 dB, during clear weather. The X-band peak efficiency of the DSS 13 antenna at f1 was determined to be 75.35 percent at an elevation angle of 45.63 degrees. This corresponds to a peak gain of 68.34 dBi at 8450 MHz.

The above efficiency value was measured in the post-holographic condition of the antenna, with the main reflector panels in their final adjustment condition. After initial acceptance of the antenna in July 1990, preliminary X-band f1 efficiency measurements were made. These measurements yielded a peak efficiency of 71.88 percent. Thus, the panel adjustment increased efficiency by 3.5 percentage points (a 0.21-dB improvement) in addition to resetting the rigging angle to near 45 deg instead of the initial 58 deg. (These values are shown in Table 8, along with the results of all other post-holographic measurements.) Figure 2 shows the pre- and post-holographic comparison. The tolerances shown in Fig. 2 include the effects of random measurement error and curve fitting methodology only. Other effects which are common to both sets of measurements (source flux and size correction) are not included, so as to emphasize the fact that the 0.21-dB improvement shown is indeed statistically significant. Figure 3 shows the X-band f1 efficiency curve along with the adjusted data points.

VII. Efficiency Measurements: X-Band at f3, November 1990

By methods similar to those described above, X-band f3 measurements were made two months later. The radio sources used were restricted to three: 3C274, 3C84, and 3C123. Atmospheric attenuation at zenith varied from 0.035 dB to 0.037 dB, a lower and smaller range than in September, undoubtedly due to lower water vapor contribution. By using 3C274 as the standard gain calibrator and the other two sources to provide shape information, it was found that the efficiency of the beam waveguide system was somewhat lower than at f1. The final peak efficiency was determined to be 72.38 percent at an elevation angle of 40.21 deg, a decrease of 2.97 percent. The corresponding f3 gain is 68.17 dBi. Table 3 gives the deduced flux and $T100/C_r$ values determined during the f3 measurements.

It is seen that the $T100/C_r$ value of 3C123 appears to have decreased 1.51 percent, and that of 3C84 appears to have decreased 2.12 percent in the two months between September and November 1990. Again, these changes are relative to 3C274, and because they are both small, they may not be significant. As 3C123 is not considered to be variable, the 1.51 percent change may be due to noise in the data.

Figure 3 shows the adjusted data points and individual curve fits for the three sources (3C123 and 3C84 adjusted). It appears that the fits for 3C123 and 3C84 are significantly different at high elevation angles (at meridian transit). Because of the different declinations of these two sources, 3C123 passes south at meridian transit and 3C84 passes north, although both are only 6 deg from zenith. It is now believed that the different efficiency values at high elevation are azimuth-related and are due to a misalignment of the ellipsoidal and flat mirrors at the bottom of the beam waveguide system. At meridian transit, these two sources have 180 deg different azimuths. Note that

3C274, which also passes south of the antenna at meridian transit (although at only 67 deg elevation), has a curve fit more like that of 3C123, which also passes south.

VIII. Efficiency Measurements: Ka-Band at f1, October 1990

The four radio sources used for Ka-band measurements were 3C274, 3C84, 3C273, and Venus. The 3C274 flux appears to be well known, as determined in a recent analysis at JPL.[1] The source size correction was calculated by integrating the antenna beam (0.017-deg beamwidth) over a frequency-extrapolated map of the source. The source-size correction thus determined was 1.273. The flux of 3C84 was unknown, but a starting value was used based on 32-GHz measurements carried out on the Goldstone 70-meter antenna (DSS 14) in 1989 [5]. In that report, a flux of 43.71 Janskys was deduced with reference to measurements made by using 3C274 and Venus as standard calibrators. It was found during the f1 measurements that this value required substantial adjustment to bring the October 1990 efficiency measurements into agreement with those determined by Venus and 3C274.

Flux from Venus was calculated from the expression given above in Section III. The source size correction, C_r, for a disk is calculated from:[2]

$$C_r = \frac{X}{1 - e^{-X}}$$

where

$X = (r^2)/(2\sigma^2)$

r = angular radius of disk, deg

$\sigma = \Theta_o/2.3548$, deg

Θ_o = full 3-dB antenna beamwidth, deg

$T100/C_r$ is calculated as usual from

$$\frac{T100}{C_r} = \frac{SA}{2kC_r}$$

as described above.

A value of 475 K was used for the blackbody disk temperature of Venus [5,6]. The planetary disk diameter of Venus used was 12,240 km [6]. During the Ka-band f1 measurement period, Venus was near superior conjunction, and the distance from Earth to Venus changed very little, from about 1.70 to 1.72 AU. Table 4 gives the values used in the Ka-band calibration at f1.

Using the Table 4 $T100/C_r$ values for the sources listed, the f1 efficiency as determined by using Venus, was found to be 51.50 percent. By using 3C274, the efficiency was found to be 53.12 percent. As both sources are regarded to be standard calibrators, the results were averaged, yielding a final f1 efficiency value of 52.31 percent at an elevation angle of 44.82 deg. The corresponding gain is 78.33 dBi. The zenith atmospheric attenuation during the measurement period ranged from 0.133 dB to 0.233 dB. Adjustments in the flux and $T100/C_r$ values of 3C84 and 3C273 were made in order to match the efficiency found above. Table 5 gives these adjustments.

It should be noted that the adjustments for 3C274 and Venus are shown as needed only to establish an average peak gain value. As the sources are considered to be standard calibrators, the adjustments do not imply new flux or $T100/C_r$ values.

Figure 4 shows the adjusted data points and the curve fit for the Ka-band f1 measurements.

IX. Efficiency Measurements: Ka-Band at f3, January 1991

Ka-band measurements at f3 during December 1990 showed a very apparent efficiency anomaly, which unfortunately became known as the "hysteresis effect," because it was initially thought to be due to a mechanical inelasticity (which turned out not to be the case). After numerous tests, it was determined that the most likely cause of this effect was a misalignment of the ellipsoidal mirror in the pedestal room. Realignment of the mirror was done in early January 1991. It was then decided to re-do the Ka-band f3 measurements throughout that month. Only Venus, 3C274, and 3C84 were used for these tests. Table 6 gives the flux and $T100/C_r$ values used during the Ka-band f3 measurements. Note that a dummy value of $T100/C_r = 10.000$ is used for 3C84 (based on 9.629 deduced at f1). The real value would be determined after comparison with the Venus and 3C274 efficiency results.

Zenith atmospheric attenuation during these tests varied from 0.096 dB to 0.120 dB, substantially lower than during the f1 tests. Weather during the tests was clear and very cold, with very low absolute humidity. Table 7

[1] P. H. Richter, *Virgo-A Flux Density*, JPL Interoffice Memorandum 3393-90-137 (internal document), Jet Propulsion Laboratory, Pasadena, California, October 18, 1990.

[2] P. H. Richter, personal communication, Jet Propulsion Laboratory, Pasadena, California, October 1, 1990.

gives the efficiency adjustments needed and the deduced values of flux and $T100/C_r$. Note that although adjustments are shown for Venus and 3C274, the given values of flux and $T100/C_r$ are not changed from the initial values given above, as they are considered to be calibration standards.

The peak Ka-band f3 efficiency was determined to be 44.89 percent at an elevation angle of 45.41 deg. This corresponds to a gain of 77.66 dBi.

Several things should be noted about Table 7. Compared with the Ka-band f1 measurements, the 3C274 and Venus adjustment directions have been reversed. The adjustment for 3C84 is based on an assumed $T100/C_r$ value of 10.000, a dummy value. The final deduced flux and $T100/C_r$ values for 3C84 vary only by 1.24 percent from those determined in the f1 measurements, even though the source is variable and three months time had elapsed. This may hint at the period of variation of the source.

Figure 4 shows the adjusted data points and the curve fits for the three calibration sources. Again, the spread of curve fits at the high elevation angles shows the effect of possible ellipsoidal mirror misalignment. Note that the mirror alignment for the Ka-band f3 tests is different from that for the X-band f3 tests in November 1990. As compared with the X-band curve fits, the southern-passing sources (3C274, Venus) straddle the curve fit of the northern-passing source (3C84), rather than being above it. Because of the low declination of Venus during the f3 tests (resulting in low peak-elevation angle), the curve fit at high elevation angles may be in error, thus giving this result.

X. Final Results

Table 8 gives a summary of the final gain and efficiency measurements described above. In addition, the estimated 1-σ errors are given, as well as shown in Figs. 3 and 4. The errors are due to source flux uncertainty, source size-correction error, data noise, curve fitting, and reduction methodology. For purposes of comparison, Fig. 5 shows all data sets and curve fits together. The frequency-dependent effect of main-reflector structural deformation is clearly seen in this figure.

Table 9 gives the coefficients of the final antenna efficiency curve-fit polynomials used in the generation of Figs. 3, 4, and 5.

Table 10 gives final radio-source flux and $T100/C_r$ values deduced from the efficiency measurements described above. When two different values have been found from f1 and f3 measurements, the value presented here is the average of the two. These values are, at least, a starting point for future measurements. In the case of standard calibrators (3C274, Venus), no new values are given. The $T100/C_r$ values given for non-point sources are valid only for use in the calibration of 34-meter diameter antennas with X- and Ka-band beamwidths of 65 and 17 mdeg, respectively. The C_r values were calculated by using these beamwidths. Care should be taken in calibration measurements when the antenna beamwidth varies from these numbers. Simple modeling is typically not accurate.

XI. Conclusion

This article has presented a complete review of the initial 8.45- and 32-GHz efficiency calibration of the new NASA Deep Space Network beam waveguide antenna at the Goldstone Deep Space Communications Complex. The novel technique of using portable test packages to evaluate antenna performance at various locations in the microwave optics path has proved to be straightforward to implement and successful in operation. At the beam waveguide focus, 8.45- and 32-GHz peak efficiencies of 72.38 and 44.89 percent, respectively, were achieved. The efficiency determinations presented here met the functional requirements of the DSS 13 project and agreed well with predictions which considered feed illumination and spillover, waveguide and mirror losses, and beam waveguide effects.

Acknowledgments

The authors wish to thank R. L. Riggs for the development of the boresight methodology and programming, without which the measurements described here would have been impossible. D. L. Brunn assisted greatly with experiment planning. P. H. Richter provided updated radio-source flux and source size-correction values. The authors are also indebted to Goldstone DSS 13 personnel for their support during the many months of the measurement program.

References

[1] J. A. Turegano and M. J. Klein, "Calibration Radio Sources for Radio Astronomy: Precision Flux Density Measurements at 8420 MHz," *Astron. Astrophys.*, vol. 86, pp. 46–49, 1980.

[2] J. A. Turegano and M. J. Klein, "Precision Flux Density Measurements of the Giant Planets at 8420 MHz," *Astron. Astrophys.*, vol. 94, pp. 91–94, 1981.

[3] P. H. Richter and S. D. Slobin, "DSN 70-Meter Antenna X- and S-Band Calibration, Part I: Gain Measurements," *TDA Progress Report 42-97*, vol. January–March 1989, Jet Propulsion Laboratory, Pasadena, California, pp. 314–351, June 15, 1989.

[4] P. H. Richter and S. D. Slobin, "Errata to DSN 70-Meter Antenna X- and S-Band Calibration, Part I: Gain Measurements," *TDA Progress Report 42-99*, vol. July–September 1989, Jet Propulsion Laboratory, Pasadena, California, p. 220, November 15, 1989.

[5] M. S. Gatti, M. J. Klein, and T. B. H. Kuiper, "32-GHz Performance of the DSS 14 70-Meter Antenna: 1989 Configuration," *TDA Progress Report 42-99*, vol. July–September 1989, Jet Propulsion Laboratory, Pasadena, California, pp. 206–219, November 15, 1989.

[6] P. G. Steffes, M. J. Klein, and J. M. Jenkins, "Observations of the Microwave Emission of Venus from 1.3 to 3.6 cm," *Icarus*, vol. 84, pp. 83–92, 1990.

Table 1. Radio sources used for 8.45-GHz (X-band) calibrations at f1 and f3, September 1990 and November 1990

Source	Declination, J2000.0	Peak Elevation at DSS 13 LAT = 35.25 deg	Flux, Jy	C_r	$T100/C_r, K$
3C274[a]	12.391	67.1	44.555	1.087	13.477
3C123[b]	29.671	84.4	9.404	1.0054	3.0753
DR21[b]	42.329	82.9	19.902	1.0085	6.489
3C84[c,d]	41.512	83.7	45.79	1.000	15.056
3C273[c]	2.052	56.8	36.46	1.000	11.988

[a] P. H. Richter, *Virgo-A Flux Density*, JPL Interoffice Memorandum 3393-90-137 (internal document), Jet Propulsion Laboratory, Pasadena, California, October 18, 1990.

[b] P. H. Richter, personal communication, Jet Propulsion Laboratory, Pasadena, California, July 26, 1990.

[c] The values as shown in [d] reduced by 0.076 dB as per [3] calibration analysis of 70-meter antenna gain, and [4].

[d] M. Klein, et al., *DSN Radio Source List for Antenna Calibration*, JPL Document D-3801, Rev. B (internal document), Jet Propulsion Laboratory, Pasadena, California, September 25, 1987.

Table 2. Efficiency adjustments, deduced flux, and *T100/Cr* values: 8.45 GHz (X-band) at f1, September 1990

Source	Efficiency Adjustment Needed	Deduced Flux, Jy	Deduced $T100/C_r, K$
3C274[a]	1.00000	44.555	13.477
3C123[b]	0.98722	—	3.115
DR21[b]	0.99478	—	6.523
3C84[c]	1.40141	32.67	10.743
3C273[c]	1.24420	29.30	9.635

[a] Extended

[b] Nonpoint

[c] Variable, point

Table 3. Efficiency adjustments, deduced flux and *T100/Cr* values: 8.45 GHz (X-band) at f3, November 1990

Source	Efficiency Adjustment Needed	Deduced Flux, Jy	Deduced $T100/C_r, K$
3C274[a]	1.00000	44.555	13.477
3C123[b]	1.00240	—	3.068
3C84[c]	1.43183	31.98	10.515

[a] Extended

[b] Nonpoint

[c] Variable, point

Table 4. Radio sources used for 32 GHz (Ka-band) calibrations at f1, October 1990

Source	Declination, J2000.0	Distance, AU	Peak Elevation at DSS 13 LAT = 35.25 deg	Flux, Jy	C_r	$T100/C_r, K$
3C274[a]	12.391		67.1	16.22	1.273	4.190
3C84[b]	41.512		83.7	43.71	1.000	14.372
3C273[b]	2.052		56.8	29.54	1.000	9.713
Venus 1990[c]						
Oct 01	+1.6	1.69539	56.4	27.323	1.00828	8.914
Oct 10	−2.9	1.70591	51.9	26.987	1.00818	8.806
Oct 20	−7.9	1.71302	46.9	26.764	1.00811	8.733
Oct 30	−12.5	1.71538	42.3	26.690	1.00809	8.709

[a] P. H. Richter, *Virgo-A Flux Density*, JPL IOM 3393-90-137 (internal document), Jet Propulsion Laboratory, Pasadena, California, October 18, 1990.

[b] M. S. Gatti, M. J. Klein, and T. B. H. Kuiper, "32-GHz Performance of the DSS 14 70-Meter Antenna; 1989 Configuration," *TDA Progress Report 42-99*, vol. July–September 1989, Jet Propulsion Laboratory, Pasadena, California, pp. 206–219, November 15, 1989.

[c] Declination of date

Table 5. Efficiency adjustments, deduced flux, and *T100/Cr* values: 32 GHz (Ka-band) at f1, October 1990

Source	Efficiency Adjustment Needed	Deduced Flux, Jy	Deduced $T100/C_r, K$
3C274[a]	0.98475	16.22	4.190
Venus[b]	1.01573	Table 4	Table 4
3C84[c]	1.49278	29.281	9.628
3C273[c]	0.94022	31.418	10.331

[a] Extended

[b] Nonpoint

[c] Variable, point

Table 6. Radio sources used for 32-GHz (Ka-band) calibrations at f3, January 1991

Source	Declination, J2000.0	Distance, AU	Peak Elevation at DSS 13 LAT = 35.25 deg	Flux, Jy	C_r	$T100/C_r, K$
3C274[a]	12.391		67.1	16.22	1.273	4.190
3C84[b,c]	41.512		83.7	—	1.000	10.000
Venus 1991[d]						
Jan 01	−22.5	1.63496	32.3	29.380	1.00891	9.579
Jan 10	−20.2	1.61115	34.6	30.255	1.00918	9.862
Jan 20	−16.8	1.58115	38.0	31.414	1.00953	10.236
Jan 30	−12.6	1.54728	42.2	32.804	1.00995	10.685

[a] P. H. Richter, *Virgo-A Flux Density*, JPL IOM 3393-90-137 (internal document), Jet Propulsion Laboratory, Pasadena, California, October 18, 1990.

[b] M. S. Gatti, M. J. Klein, and T. B. H. Kuiper, "32-GHz Performance of the DSS 14 70-Meter Antenna; 1989 Configuration;" *TDA Progress Report 42-99*, vol. July–September 1989, Jet Propulsion Laboratory, Pasadena, California, pp. 206–219, November 15, 1989.

[c] Dummy value for $T100/C_r$ based on 9.628 found at f1.

[d] Declination of date

Table 7. Efficiency adjustments, deduced flux, and *T100/Cr* values: 32 GHz (Ka-band) at f3, January 1991

Source	Efficiency Adjustment Needed	Deduced Flux, Jy	Deduced $T100/C_r, K$
3C274[a]	1.03417	16.22	4.190
Venus[b]	0.96804	Table 6	Table 6
3C84[c]	1.02592	29.643	9.747

[a] Extended

[b] Variable

[c] Variable, point

Table 8. DSS BWG antenna X- and Ka-band final peak gains and efficiencies

	Gain, dBi	Efficiency, percent
8.45 GHz, X-band		
f1 pre-holography at 58.03 deg elevation	68.14	71.88
f1 post-holography at 45.63 deg elevation	68.34	75.35
f3 post-holography at 40.21 deg elevation	68.17	72.38
Estimated 1-σ errors	0.14 dB	2.3
32 GHz, Ka-band		
f1 post-holography at 44.82 deg elevation	78.33	52.31
f3 post-holography at 45.41 deg elevation	77.66	44.89
Estimated 1-σ errors	0.33 dB	3.6

Table 9. Coefficients of polynomial expressions for DSS 13 BWG antenna X- and Ka-band efficiencies without atmosphere

Efficiency	Efficiency, without atmosphere $= a_0 + a_1\theta + a_2\theta^2$ where θ = antenna elevation angle, degrees		
	a_0	a_1	a_2
X-band at f1	0.72734	0.00114701	−0.0000125694
X-band at f3	0.68496	0.00192912	−0.0000239880
Ka-band at f1	0.27220	0.01119613	−0.0001249108
Ka-band at f3	0.18285	0.01171770	−0.0001290241

Table 10. Final radio source flux and *T100/Cr* values deduced from DSS 13 34-m antenna-efficiency measurements

Frequency	Source	Flux, Jy	C_r	$T100/C_r$
8.45 GHz X-band	3C274[a,b]	44.555	1.087	13.477
	3C123[b]	—	—	3.092
	DR21[c]	—	—	6.523
	3C84[b,d]	32.67	1.000	10.629
	3C273[c,d]	29.30	1.000	9.635
32 GHz Ka-band	3C274[a,b]	16.22	1.273	4.190
	3C84[b,d]	29.462	1.000	9.688
	3C273[c]	31.418	1.000	10.331
	Venus[a,b,d]		—see text—	

[a] Calibration standard, no new values deduced

[b] f1 and f3 measurements

[c] f1 measurement only

[d] Variable source

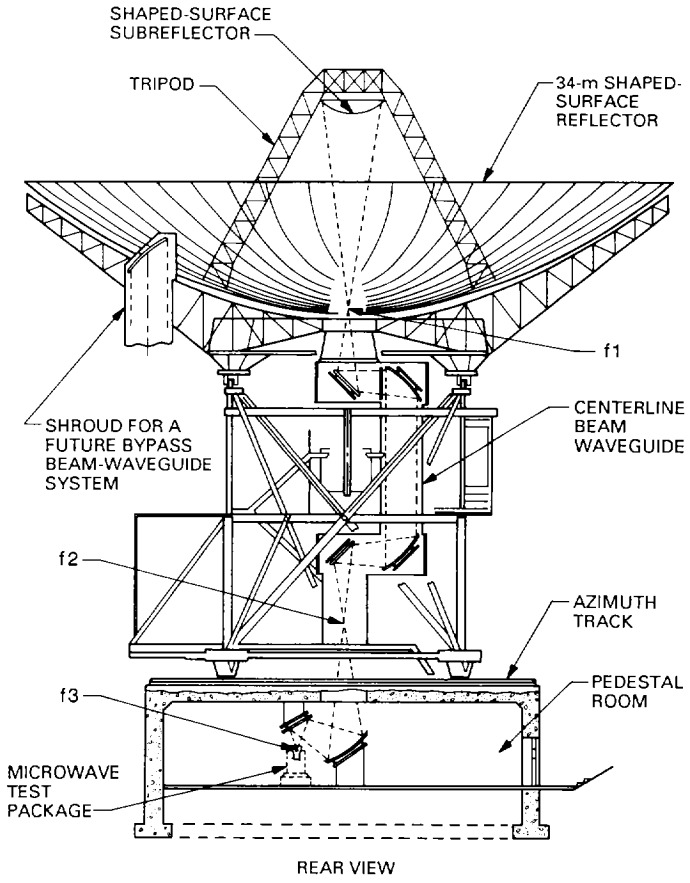

Fig. 1. Mechanical and microwave optics designs of NASA/JPL DSN beam waveguide antenna at Goldstone, DSS 13.

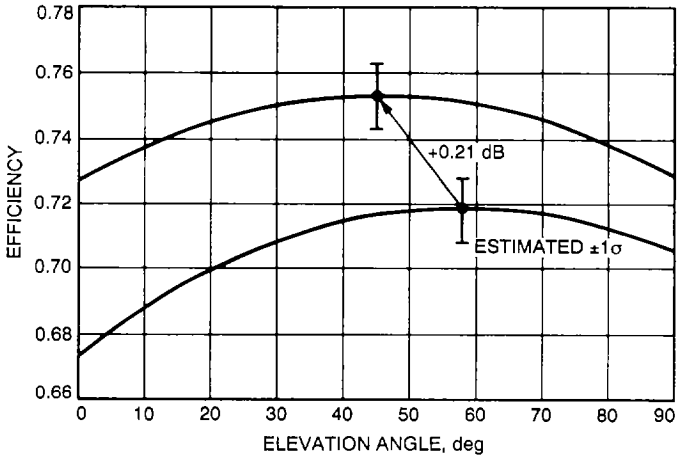

Fig. 2. DSS 13 8.45 GHz (X-band) efficiency at f1, pre-holography (bottom) and post-holography (top), without atmosphere.

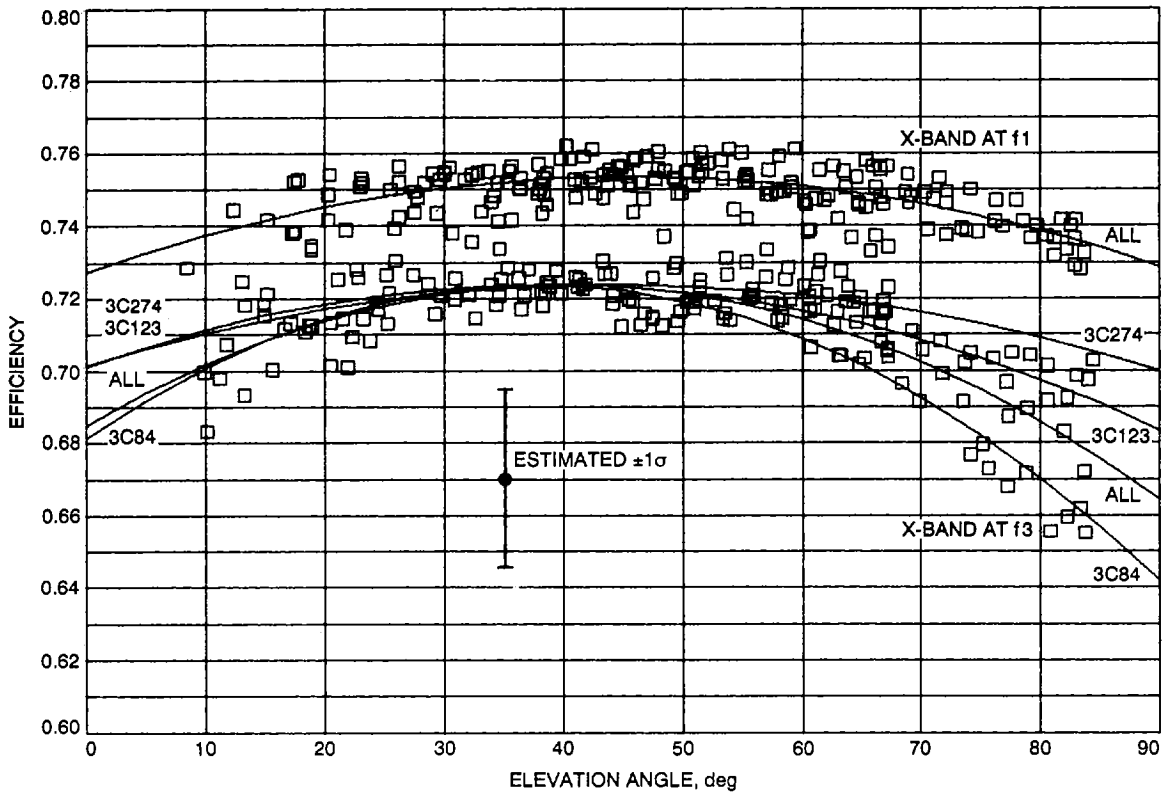

Fig. 3. DSS 13 8.45 GHz (X-band) efficiency at f1 and f3 focal points, without atmosphere.

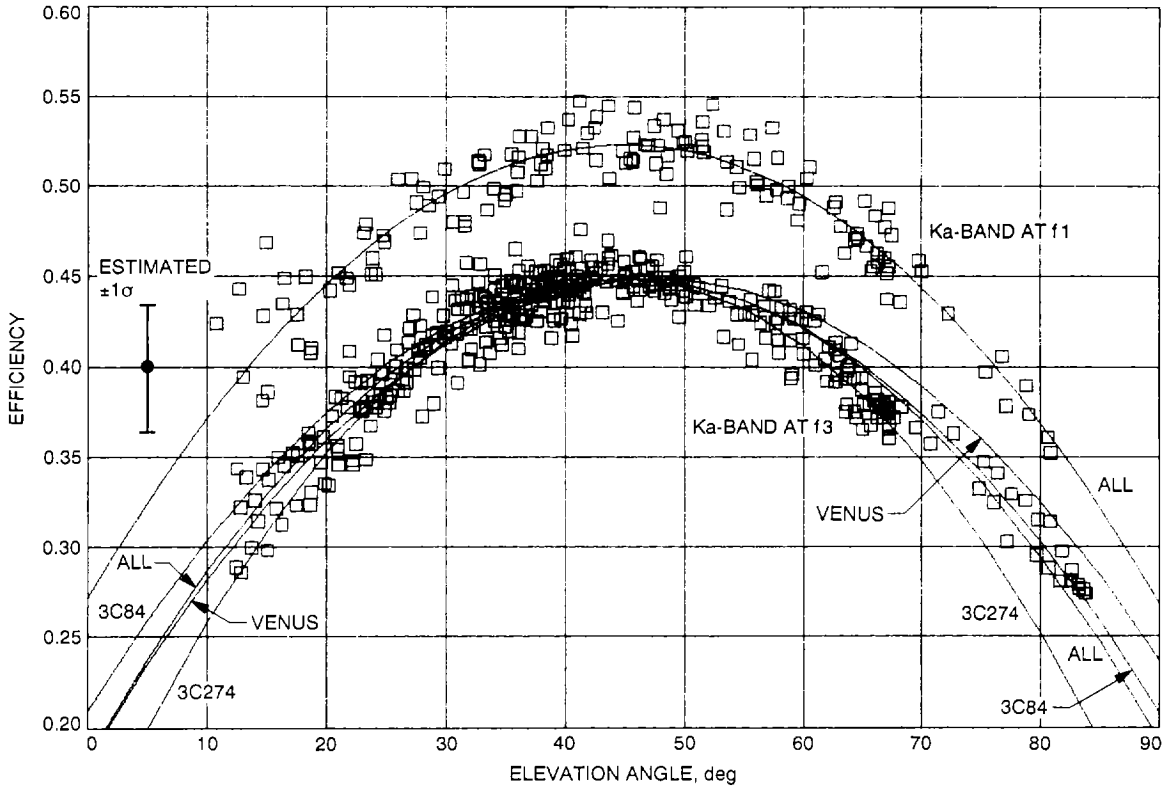

Fig. 4. DSS 13 32 GHz (Ka-band) efficiency at f1 and f3 focal points, without atmosphere.

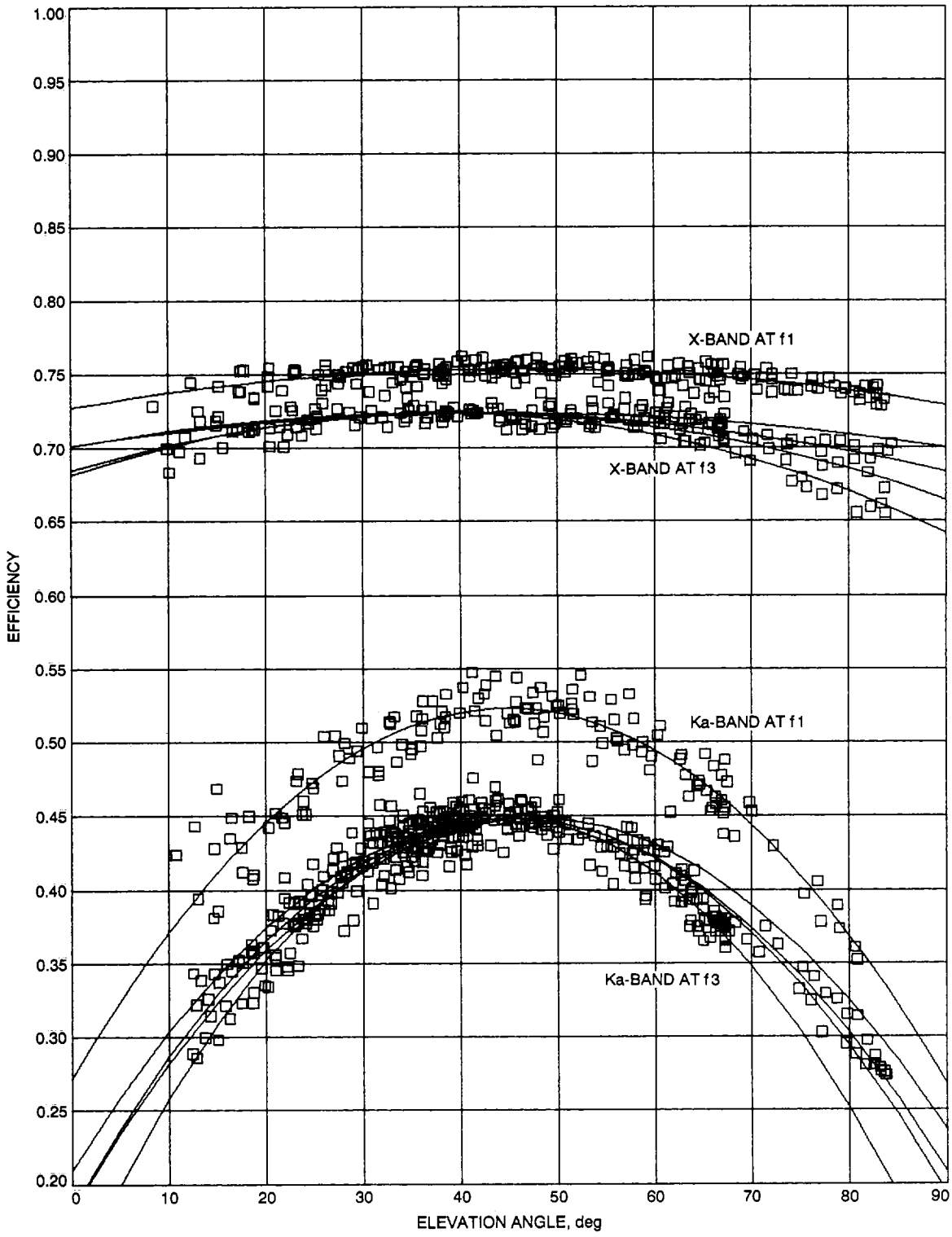

Fig. 5. DSS 13 X- and Ka-band efficiencies at f1 and f3 focal points, without atmosphere.